Erfonium: A Hooke Atom with Soft Interaction Potential*

Jacek Karwowski

Institute of Physics, Faculty of Physics,

Astronomy and Informatics,

Nicolaus Copernicus University,

Grudziądzka 5, 87-100 Toruń, Poland

email: jka@umk.pl

Andreas Savin

Laboratoire de Chimie Théorique,

CNRS and Sorbonne University,

4 place Jussieu, 75252 Paris cedex 05, France

email: andreas.savin@lct.jussieu.fr

Abstract

Properties of *erfonium*, a Hooke atom with the Coulomb interaction potential $1/r$ replaced by a non-singular $\mathrm{erf}(\mu\, r)/r$ potential are investigated. The structure of the Hooke atom potential and properties of its energy spectrum, relative to the ones of the spherical harmonic oscillator and of harmonium, are analyzed. It is shown, that at a certain value of μ the system changes its behavior from a harmonium-like regime to a harmonic-oscillator-like regime.

Keywords: Schrödinger equation, electron interaction, Hooke atoms, erf potential, range separation.

* This is a preprint of the following chapter: Jacek Karwowski and Andreas Savin, A Hooke Atom with Soft Interaction Potential, published in Recent Progress in Methods and Applications of Quantum Systems, edited by Ireneusz Grabowski, Karolina Słowik, Erkki J. Brändas, and Jean Maruani, 2023, Springer Nature, reproduced with permission of Springer Nature Switzerland AG Gewerbestrasse 11, 6330 Cham, Switzerland. The final authenticated version is available online at: xxxxx.

I. MOTIVATION

The interaction between electrons can be split to two parts:

$$\frac{1}{r} = \frac{\mathrm{erf}(\mu\, r)}{r} + \frac{\mathrm{erfc}(\mu\, r)}{r}. \tag{1}$$

The first, long-range, term is smooth at $r \sim 0$ and behaves as the Coulomb potential at $r \to \infty$. The second, short-range one, correctly represents the Coulomb potential at small r and decays exponentially as $r \to \infty$. From this observation stems the concept of range separation [1–3], where the long-range section and the short-range section are treated in different ways.

In theories of many-electron systems, the replacement of the singular Coulomb potential by a smooth long-range potential, signifficantly reduces the computational effort. On the other hand, the short-range behavior of the wave function is mostly defined by the universal properties of the Coulomb singularity. Therefore the idea of improving models which utilize the long-range interactions only, by some universal corrections describing the short-range properties is very tempting. Indeed, correcting solutions of the Schrödinger equation with the long-range part of the interaction potential, by using the generalized cusp conditions to represent the wave functions in the small r area, was recently shown not only feasible, but also very accurate [4].

The long-range Coulomb interaction potentials,

$$\mathsf{w}(r;\mu) = \frac{\mathrm{erf}(\mu\, r)}{r}, \tag{2}$$

have been introduced in several areas of chemistry and physics. For example, a model with the Coulomb interaction replaced by $\mathsf{w}(r;\mu)$ correctly reproduces some selected properties of the hydrogen atom, harmonium, and electron gas [5]. In quantum chemistry, the replacement of the singular Coulomb potential by a smooth one represented by the error function is particularly convenient with the Gaussian basis sets: the integrals with this potential are easy to calculate. Therefore, the applications of the range separation concept, though most common in the density functional theory [2, 6], extend beyond this field [3].

Also in theory of complex systems, as crystals, liquids, or plasmas, using $\mathrm{erf}(\mu\, r)/r$ potential is motivated by its mathematical properties. Probably for the first time it was used by Ewald in 1921, well before the formulation of quantum mechanics, to replace the Coulomb

interaction in order to secure the convergence of some series describing infinite systems of particles [7]. A reader interested in these areas of applications is referred to a recent paper [8], where also references to the earlier works are supplied. Due to its convenient mathematical form and simple relation to the Coulomb potential, $\mathrm{erf}(\mu\, r)/r$ potential is also used in many other sections of physics, just to mention so distant fields as interactions between quarks [9], or general theory of relativity [10].

Two electrons with interaction represented by $\mathsf{v}(r)$, in an external potential $\mathsf{W}(\boldsymbol{r}_1)+\mathsf{W}(\boldsymbol{r}_2)$, are described by the Hamiltonian

$$\mathsf{H}(\boldsymbol{r}_1,\boldsymbol{r}_2) = -\tfrac{1}{2}\,\triangle_{\boldsymbol{r}_1} - \tfrac{1}{2}\,\triangle_{\boldsymbol{r}_2} + \mathsf{W}(\boldsymbol{r}_1) + \mathsf{W}(\boldsymbol{r}_2) + \mathsf{v}(r), \tag{3}$$

where $r = |\boldsymbol{r}| \equiv |\boldsymbol{r}_1 - \boldsymbol{r}_2|$. Introducing $\boldsymbol{R} = (\boldsymbol{r}_1 + \boldsymbol{r}_2)\,/2$ we get

$$\boldsymbol{r}_1 = \boldsymbol{R} + \tfrac{1}{2}\,\boldsymbol{r}, \quad \boldsymbol{r}_2 = \boldsymbol{R} - \tfrac{1}{2}\,\boldsymbol{r}. \tag{4}$$

If $\mathsf{W}(\boldsymbol{r}_i) \;\propto\; r_i^2$, $i = 1, 2$, then the Hamiltonian is separable and the two-electron eigenvalue equation splits to two spherically-symmetric equations [11]. The first one, in $\boldsymbol{R}$, is independent of the interaction potential, and describes the motion of the center of mass of two electrons in the parabolic confining potential. The second equation, in $\boldsymbol{r}$, describes the relative motion of two interacting electrons in the confining potential $(\omega\, r/2)^2$, where parameter ω defines the strength of the confinement. We assume that the interaction potential is equal to $\mathsf{w}(r;\mu)$, defined in (2). The resulting model potential reads

$$\mathsf{V}(r) \;\equiv\; \mathsf{V}(r;\omega,\mu) \;=\; \frac{\mathrm{erf}(\mu\, r)}{r} + \Big(\frac{\omega\, r}{2}\Big)^2. \tag{5}$$

The elimination of the angular dependence from the second equation gives an infinite set of radial equations labelled by the angular momentum quantum number ℓ

$$\mathsf{H}(r;\ell,\omega,\mu)\,\phi_{n,\ell}(r) = E_{n,\ell}(\omega,\mu)\,\phi_{n,\ell}(r), \quad n,\ell = 0,1,2,\ldots, \tag{6}$$

where $\phi_{n,\ell}(r) = r\,\psi_{n,\ell}(r)$ is the reduced radial function, $\psi_{n,\ell}(r)$ is the radial part of the one-particle wave function, and

$$\mathsf{H}(r;\ell,\omega,\mu) = \left(-\frac{d^2}{dr^2} + \frac{\ell(\ell+1)}{r^2} + \mathsf{V}(r;\omega,\mu)\right) \tag{7}$$

is the radial Hamiltonian.

If the interaction potential $\mathsf{v}(r)$ is repulsive then its energy spectrum is continuous. The introduction of a parabolic confinement leads to the discretization of the spectrum. Two confined electrons form a bound system which resembles a two-electron atom. It is referred to as a Hooke atom (due to the confining Hooke force). If the two particles interact by the Coulomb potential, the system is called *harmonium*. We propose here the name *erfonium* for a Hooke atom with the Coulomb interatcion between electrons replaced by $\mathsf{w}(r;\mu)$. Erfonium is a generalization and unification of two well-studied systems: the spherical harmonic oscillator and harmonium. Its radial Hamiltonian (7) transforms to the Hamiltonian of the spherical harmonic oscillator if $\mu = 0$, and to the Hamiltonian of harmonium, if $\mu \to \infty$ (10). Accordingly, at these two limits the eigenvalues $E_{n,\ell}(\omega,\mu)$, and other quantities characterizing the system, approach the corresponding quantities of the harmonic oscillator and of harmonium. They are marked hereafter by superscripts $^{\mathrm{o}}$ and $^{\mathrm{h}}$, respectively.

The close relation between the Coulomb and $\mathsf{w}(r;\mu)$ potentials can be seen by comparig their integral representations. We have

$$\frac{1}{r} = \frac{2}{\sqrt{\pi}} \int_0^\infty \mathrm{e}^{-(x\,r)^2}\, dx \qquad \text{and} \qquad \frac{\mathrm{erf}(\mu\, r)}{r} = \frac{2}{\sqrt{\pi}} \int_0^\mu \mathrm{e}^{-(x\,r)^2}\, dx. \tag{8}$$

Then,

$$\frac{1}{r} \;=\; \lim_{\mu\to\infty} \frac{\mathrm{erf}(\mu\, r)}{r} \tag{9}$$

and at the limit of large μ the model potential (5) transforms to the potential of harmonium:

$$\mathsf{V}(r;\omega,\mu) \underset{\mu\to\infty}{\to} \mathsf{V}^{\mathrm{h}}(r;\omega) = \frac{1}{r} + \left(\frac{\omega\, r}{2}\right)^2. \tag{10}$$

The ℓ-dependent term in equation (7) describes the centrifugal force, and together with the model potential is called the effective radial potential:

$$\mathcal{V}(r;\ell,\omega,\mu) \;=\; \frac{\ell(\ell+1)}{r^2} + \mathsf{V}(r;\omega,\mu). \tag{11}$$

Notice, that the parameter μ in $\mathcal{V}(r;\ell,\omega,\mu)$ describes the adiabatic connection between spherical harmonic oscillator $[\mathcal{V}(r;\ell,\omega,0)]$, and harmonium $[\mathcal{V}(r;\ell,\omega,\infty)]$.

For $\ell = 0$, $\mathcal{V}(r;\ell,\omega,\mu)$ is equal to the model potential (5):

$$\mathcal{V}(r;0,\omega,\mu) \;=\; \mathsf{V}(r;\omega,\mu). \tag{12}$$

But, for $l > 0$ these two potentials are notably different. The most significant difference is in the area of small r. At $r = 0$,

$$\lim_{r\to 0} \mathcal{V}(r;0,\omega,\mu) \;=\; \lim_{r\to 0} \mathsf{V}(r;\omega,\mu) = \frac{2\,\mu}{\sqrt{\pi}}, \tag{13}$$

while

$$\mathcal{V}(r;\ell,\omega,\mu) \underset{r\to 0}{\sim} \frac{\ell\,(\ell+1)}{r^2} \tag{14}$$

i.e. it is singular if $\ell \neq 0$.

This paper is aimed at the exploration of some general properties of erfonium. General characteristics of the model potential (5) are presented in the next section. The effective radial potential (11) is discussed in section 3. The energy spectrum of erfomium is analyzed in section 4. Final remarks complete the work. All equations and numerical values are here expressed in the Hartree atomic units.

II. THE MODEL POTENTIAL

The radial potential of erfonium (5) can be expressed as

$$\mathsf{V}(r;\omega,\mu) \;=\; \mu\,\left[\frac{\mathrm{erf}(\mu\,r)}{(\mu\,r)} + \frac{2\,q}{3\,\sqrt{\pi}}(\mu\,r)^2\right] \tag{15}$$

$$\;=\; \frac{2\mu}{\sqrt{\pi}}\left[1 - \frac{(1-q)}{3\cdot 1!}(\mu\,r)^2 + \frac{(\mu\,r)^4}{5\cdot 2!} - \frac{(\mu\,r)^6}{7\cdot 3!} + \cdots\right] \tag{16}$$

where

$$q = \frac{3\omega^2\sqrt{\pi}}{8\,\mu^3}. \tag{17}$$

Potential $\mathsf{V}(r;\omega,\mu)$ has interesting scaling properties. According to equation (15)

$$\mathsf{V}(r/\mu;\omega,\mu) = \mu\,\left(\frac{\mathrm{erf}(r)}{r} + \frac{2\,q}{3\,\sqrt{\pi}}\,r^2\right). \tag{18}$$

As we can see, all potentials with the same value of q have exactly the same shape - they only differ by units in which V and r are expressed. Therefore, for an arbitrary pair (μ_1,μ_2)

$$\frac{\mathsf{V}(r/\mu_1;\omega_1,\mu_1)}{\mathsf{V}(r/\mu_2;\omega_2,\mu_2)} = \frac{\mu_1}{\mu_2} \tag{19}$$

if

$$\omega_2 = \omega_1\,\left(\frac{\mu_2}{\mu_1}\right)^{3/2}, \tag{20}$$

i.e. if the cofinement parameters ω_1 and ω_2 are related to μ_1 and μ_2 as

$$\left(\frac{\omega_1}{\omega_2}\right)^2 = \left(\frac{\mu_1}{\mu_2}\right)^3. \tag{21}$$

For example, the potential energy curve corresponding to ($\mu = 1$, $\omega = 1$) is, except for scaling, the same as the curve for ($\mu = 10^{-2/3} \approx 0.2154$, $\omega = 0.1$) or for ($\mu = 100^{-2/3} \approx$

0.0464, $\omega = 0.01$). From equation (18) we can get similar scaling relations for the derivatives of V with respect to r:

$$\frac{\mathsf{V}^{(n)}(r/\mu_1;\omega_1,\mu_1)}{\mathsf{V}^{(n)}(r/\mu_2;\omega_2,\mu_2)} = \left(\frac{\mu_1}{\mu_2}\right)^{n+1}, \tag{22}$$

where $\mathsf{V}^{(n)}$ is the n-th derivative of V with respect to r.

The first and the second derivatives of $\mathsf{V}(r;\omega,\mu)$ are expressed as

$$\mathsf{V}'(r;\omega,\mu) = \mu^2\left[-\frac{\mathrm{erf}(\mu\,r)}{(\mu\,r)^2}+\frac{2}{\sqrt{\pi}}\frac{\mathrm{e}^{-(\mu\,r)^2}}{(\mu\,r)}+\frac{4\,q}{3\sqrt{\pi}}(\mu\,r)\right] \tag{23}$$

$$= \frac{2\,\mu^2}{\sqrt{\pi}}\left[-\frac{2\,(1-q)}{3\cdot 1!}(\mu\,r)+\frac{4}{5\cdot 2!}(\mu\,r)^3-\frac{6}{7\cdot 3!}(\mu\,r)^5+\cdots\right]; \tag{24}$$

$$\mathsf{V}''(r;\omega,\mu) = -\frac{2}{r}\frac{d\mathsf{V}(r;\omega,\mu)}{dr}-\mu^3\frac{4}{\sqrt{\pi}}\left(\mathrm{e}^{-(\mu\,r)^2}-q\right) \tag{25}$$

$$= \frac{2\,\mu^3}{\sqrt{\pi}}\left[-\frac{2\,(1-q)}{3\cdot 1!}+\frac{3\cdot 4}{5\cdot 2!}(\mu\,r)^2-\frac{5\cdot 6}{7\cdot 3!}(\mu\,r)^4+\cdots\right]. \tag{26}$$

For finite μ, $\mathsf{V}'(0;\omega,\mu)=0$, and the potential has an extremum at $r=0$ – a minimum if $q>1$ and a maximum if $q<1$ [cf. equations (24) and (26)]. If $q\neq 1$ then for small r, the potential is a quadratic function of r. If $q=1$ then, at $r\sim 0$, the dependence on r is quartic. The threshold value of μ corresponding to $q=1$ is equal to

$$\mu_0(\omega) = \frac{1}{2}\left(3\sqrt{\pi}\omega^2\right)^{1/3}. \tag{27}$$

Then, $\mathsf{V}(r;\omega,\mu)$ at $r=0$ has a minimum if $\mu<\mu_0(\omega)$ and a maximum if $\mu>\mu_0(\omega)$. If $\mu\to\infty$ then, for $r\to 0$, $\mathsf{V}\sim 1/r$. Potential $\mathsf{V}(r;\omega,\mu)$ grows up to infinity with increasing r. Therefore, a maximum at $r=0$ implies the existence of a minimum at $r=r_{\mathrm{e}}(\omega,\mu)\equiv r_{\mathrm{e}}>0$. In the case of harmonium,

$$r_{\mathrm{e}}^{\mathrm{h}} \equiv r_{\mathrm{e}}^{\mathrm{h}}(\omega) = \lim_{\mu\to\infty} r_{\mathrm{e}}(\omega,\mu) = \left(\frac{2}{\omega^2}\right)^{1/3}, \tag{28}$$

$$\mathsf{V}_{\mathrm{e}}^{\mathrm{h}} \equiv \mathsf{V}_{\mathrm{e}}^{\mathrm{h}}(\omega) = \lim_{\mu\to\infty}\mathsf{V}(r_{\mathrm{e}}^{\mathrm{h}};\omega,\mu) = \frac{3}{4}\left[\omega\,r_{\mathrm{e}}^{\mathrm{h}}(\omega)\right]^2 = \frac{3}{4}\,(2\,\omega)^{2/3}, \tag{29}$$

[12, 13]. Notice that

$$\mu_0(\omega)\,r_{\mathrm{e}}^{\mathrm{h}}(\omega) = \left(\frac{3\sqrt{\pi}}{4}\right)^{1/3} \equiv \alpha \tag{30}$$

is independent of ω.

For a finite μ, the requirement that $\mathsf{V}'(r_{\rm e};\omega,\mu)=0$ yields:

$$\widetilde{r}_{\rm e}^{\,3} = {\rm erf}(\mu\, r_{\rm e}) - \frac{2\,\mu\, r_{\rm e}}{\sqrt{\pi}}\,{\rm e}^{-(\mu\, r_{\rm e})^2}, \tag{31}$$

where

$$\widetilde{r}_{\rm e} \equiv \widetilde{r}_{\rm e}(\omega,\mu) = \frac{r_{\rm e}(\omega,\mu)}{r_{\rm e}^{\rm h}(\omega)} = r_{\rm e}(\omega,\mu)\,\left(\frac{\omega^2}{2}\right)^{1/3}$$

is the normalized coordinate of the minimum. Notice, that rhs of equation (31) is equal to 0 if $\mu = 0$ and approaches 1 if $\mu \to \infty$. Its derivative with respect to $x = \mu\, r_{\rm e}$ is $(4\,x^2/\sqrt{\pi})\,{\rm e}^{-x^2} > 0$. Therefore, with increasing μ, $r_{\rm e}$ monotonically increases from 0 to $r_{\rm e}^{\rm h}$. The dependence of $\widetilde{r}_{\rm e}$ on μ, obtained by numerical solving equation (31), is presented, for several values of omega, in the upper left panel of Fig. 1.

Using equation (30) we can rewrite equation (31) as

$$\widetilde{r}_{\rm e}^{\,3} \;=\; {\rm erf}(\widetilde{\mu}\,\widetilde{r}_{\rm e}\,\alpha) - \frac{2\,\widetilde{\mu}\,\widetilde{r}_{\rm e}\,\alpha}{\sqrt{\pi}}\,{\rm e}^{-(\widetilde{\mu}\,\widetilde{r}_{\rm e}\,\alpha)^2}, \tag{32}$$

where

$$\widetilde{\mu} \equiv \widetilde{\mu}(\omega) = \frac{\mu}{\mu_0(\omega)}.$$

Equation (32) shows, that the relation between $\widetilde{r}_{\rm e}$ and $\widetilde{\mu}$ is independent of ω. It is plotted in the upper right panel of Fig. 1.

As one can see consulting equations (15) and (23),

$$\mathsf{V}_{\rm e} \equiv \mathsf{V}_{\rm e}(\omega,\mu) \equiv \mathsf{V}(r_{\rm e};\omega,\mu) = \frac{3}{4}\,(\omega\, r_{\rm e})^2 + \frac{2\mu}{\sqrt{\pi}}\,{\rm e}^{-(\mu\, r_{\rm e})^2}. \tag{33}$$

The normalized potential at its minimum is defined as

$$\widetilde{\mathsf{V}}_{\rm e} \equiv \widetilde{\mathsf{V}}_{\rm e}(\omega,\mu) = \frac{\mathsf{V}_{\rm e}(\omega,\mu)}{\mathsf{V}^{\rm h}(\omega)}. \tag{34}$$

Using equations (29), (30), and (33), we get

$$\widetilde{\mathsf{V}}_{\rm e} = \widetilde{r}_{\rm e}^{\,2} + \frac{\widetilde{\mu}}{\alpha^2}{\rm e}^{-(\widetilde{\mu}\,\widetilde{r}_{\rm e})^2}. \tag{35}$$

Since $\widetilde{r}_{\rm e}$, as a function of $\widetilde{\mu}$, is ω-independent, equation (35) implies that also the relation between $\widetilde{\mathsf{V}}_{\rm e}$ and $\widetilde{\mu}$ does not depend on ω. Plots of $\widetilde{\mathsf{V}}_{\rm e}$ versus μ, for three values of ω are presented in the lower left panel of Fig. 1. The three curves collapse into one in the lower right panel where they are plotted against $\widetilde{\mu}(\omega)$.

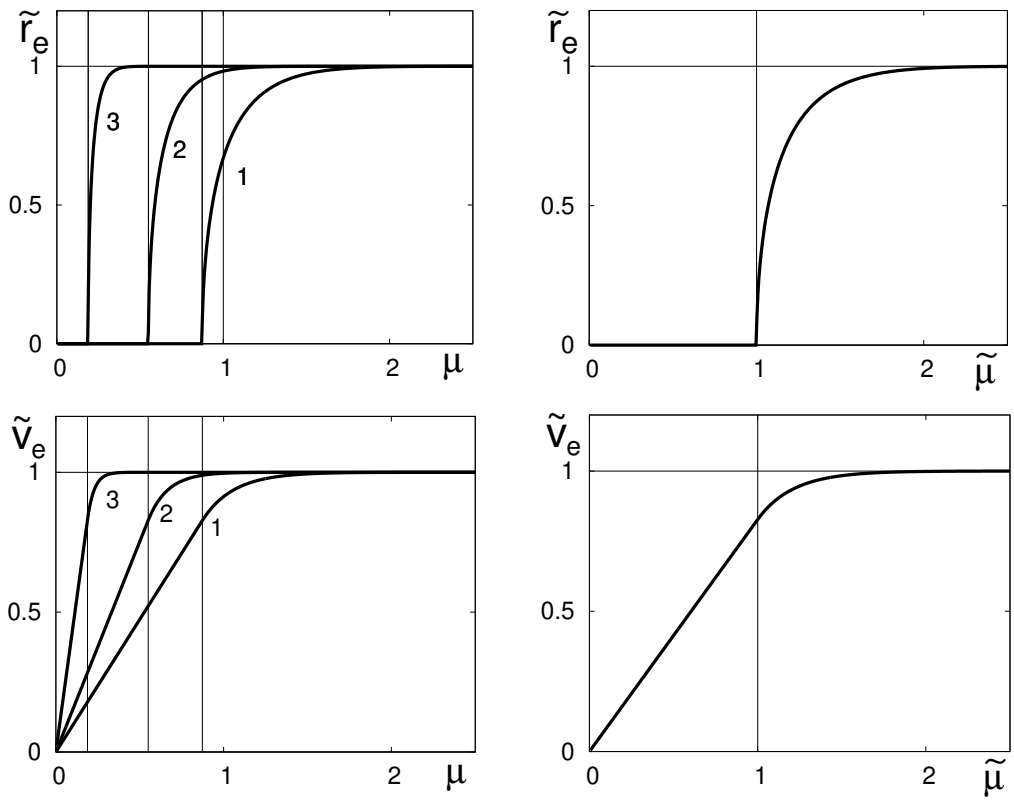

FIG. 1. Plots of $\widetilde{r}_{\rm e}(\omega,\mu)$ (top row) and $\widetilde{\mathsf{V}}_{\rm e}(\omega,\mu)$ (bottom row) versus μ (left column) and versus $\widetilde{\mu}$ (right column). Curves 1, 2, 3, correspond, respectively, to $\omega = 1.0, 0.5, 0.1$. The vertical lines mark $\mu_0(1.0) \approx 0.8727$, $\mu_0(0.5) \approx 0.5498$, and $\mu_0(0.1) \approx 0.1880$. In the right panels the curves overlap: $\widetilde{r}_{\rm e}(\omega,\widetilde{\mu})$ and $\widetilde{\mathsf{V}}_{\rm e}(\omega;\widetilde{\mu})$ are the same for all values of ω. The parameter μ is expressed in bohrs^{-1}.

Plots of $\mathsf{V}(r;\omega,\mu)$ for $\omega = 1.0$ and for $\omega = 0.1$ are shown in Fig. 2. As one can see, the curves correspnding to large μ are close to the potential of harmonium and the ones corresponding to small μ to the potential of the spherical harmonic oscillator. The shapes of the left- and of the right-panel potentials ($\omega = 1$ and $\omega = 0.1$, respectively), are the same, but the ranges of units differ by the scaling factor $100^{1/3} = 4.6416$.

Similarities and differences between erfonium and harmonium potentials are well reflected by their ratio:

$$R_0(r;\omega,\mu) = \frac{\mathsf{V}(r;\omega,\mu)}{\mathsf{V}^{\rm h}(r;\omega)} = \frac{\mathrm{erf}(\mu\, r) + \omega^2\, r^3/4}{1 + \omega^2\, r^3/4}. \tag{36}$$

If $\ell = 0$ then, for given ω and μ, the ratio is an increasing function of r. At the limit of $r \to \infty$, or $\mu \to \infty$, or $\omega \to \infty$, the ratio is equal to 1. If $r = 0$, or $\mu = \omega = 0$, then $R_0 = 0$.

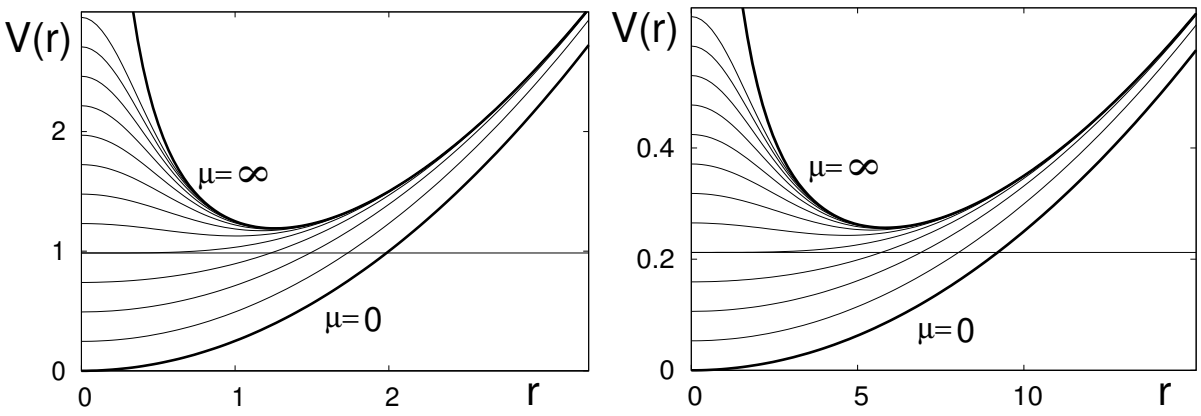

FIG. 2. Potentials $\mathsf{V}(r) \equiv \mathsf{V}(r;\omega,\mu)$, in hartrees, versus r, in bohrs. Left panel: $\omega = 1.0$ [$\mu_0(1.0) = 0.8727$]; right panel $\omega = 0.1$ [$\mu_0(0.1) = 0.1880$]. Thick lines: spherical harmonic oscillator ($\mu = 0$), and harmonium ($\mu = \infty$). Thin lines: $\mathsf{V}(r;\omega,\mu_n)$, $\mu_n = \mu_0(\omega)\cdot(n/4)$, $n = 1,\ldots,12$. The horizontal lines correspond to $q = 1$, i.e. to $\mathsf{V}(0) = 2\,\mu_0(\omega)/\sqrt{\pi}$.

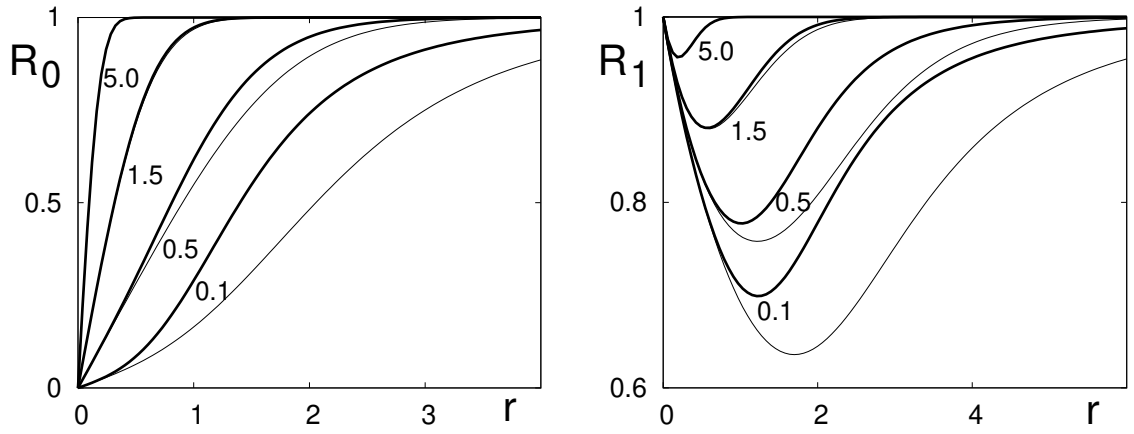

FIG. 3. Ratio of potentials of erfonium and harmonium versus r (in bohrs) for $\ell = 0$ (left panel) and for $\ell = 1$ (right panel). Thick lines - $\omega = 1.0$; thin lines - $\omega = 0.5$. The lines are marked by the values of $\mu =$ 0.1, 0.5, 1.5, 5.0. If $\mu > 1$ then the lines corresponding to different ω overlap.

Plots of $R_0(r;\omega,\mu)$ versus r, for several values of ω and μ are shown in the left panel of Fig. 3. As one can see, the ω-dependence is essential for small values of μ only. One can also notice a fast convergence of $\mathsf{V}(r;\omega,\mu)$ to $\mathsf{V}^{\rm h}(r;\omega)$ with increasing μ.

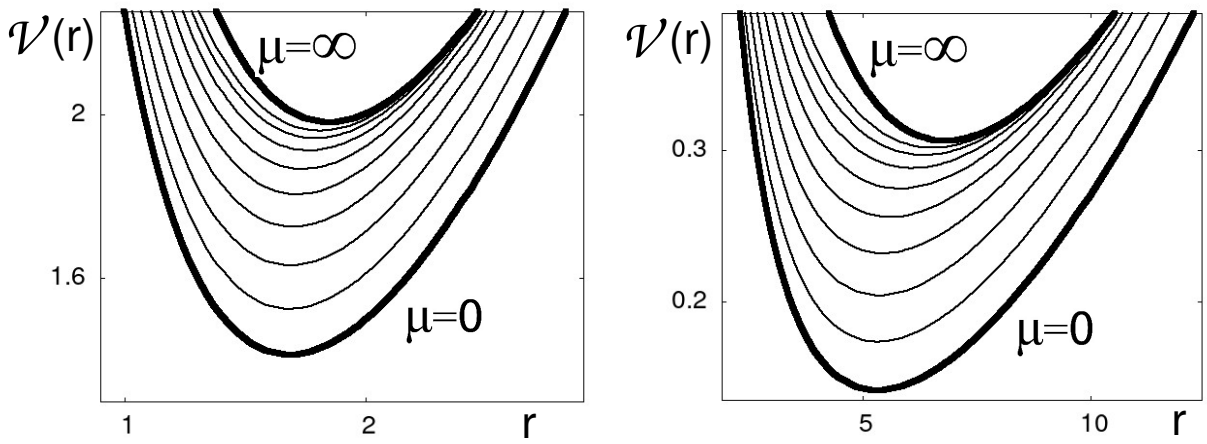

FIG. 4. The effective potential $\mathcal{V}(r) \equiv \mathcal{V}(r;\ell,\omega,\mu)$ (in hartrees) for $\ell = 1$, as functions of the inter-electronic distance r (in bohrs). Left panel - $\omega = 1.0$; right panel - $\omega = 0.1$. The lowest curves represent the effective potentials of the spherical harmonic oscillator ($\mu = 0$), and the upper ones of harmonium ($\mu = \infty$). The curves between these two limits correspond to $\mu = n/10$ (left), and $\mu = n/35$ (right), for $n = 1, \ldots, 8$.

III. THE EFFECTIVE POTENTIAL

The shape of $\mathcal{V}(r;\ell,\omega,\mu)$, similarly as the shape of $\mathsf{V}(r;\omega,\mu)$, is conserved under some specific transformations. Equation (11) can be rewritten as

$$\mathcal{V}(r/\mu;\ell,\omega,\mu) = \mu\left[\frac{\Lambda}{r^2} + \frac{\mathrm{erf}(r)}{r} + \frac{\omega^2\, r^2}{4\,\mu^3}\right], \tag{37}$$

where $\Lambda = \ell\,(\ell+1)\,\mu$. Then,

$$\frac{\mathcal{V}(r/\mu_1;\ell_1,\omega_1,\mu_1)}{\mathcal{V}(r/\mu_2;\ell_2,\omega_2,\mu_2)} = \frac{\mu_1}{\mu_2} \tag{38}$$

if

$$\left(\frac{\omega_1}{\omega_2}\right)^2 = \left(\frac{\mu_1}{\mu_2}\right)^3, \quad \text{and} \quad \Lambda_1 = \Lambda_2, \tag{39}$$

[compare eq. (21)]. This means, that two effective potentials have the same shape if,

$$\mu_2 = \mu_1\,\frac{\ell_1(\ell_1+1)}{\ell_2(\ell_2+1)}, \quad \text{and} \quad \omega_2 = \omega_1\left[\frac{\ell_1(\ell_1+1)}{\ell_2(\ell_2+1)}\right]^{3/2} \tag{40}$$

As it follows from equations (10) and (11)

$$\mathcal{V}(r;\ell,\omega,\mu) \underset{\mu\to\infty}{\to} \mathcal{V}^{\mathrm{h}}(r;\ell,\omega) \quad \text{and} \quad \mathcal{V}(r;\ell,\omega,\mu) \underset{\mu\to 0}{\to} \mathcal{V}^{\mathrm{o}}(r;\ell,\omega), \tag{41}$$

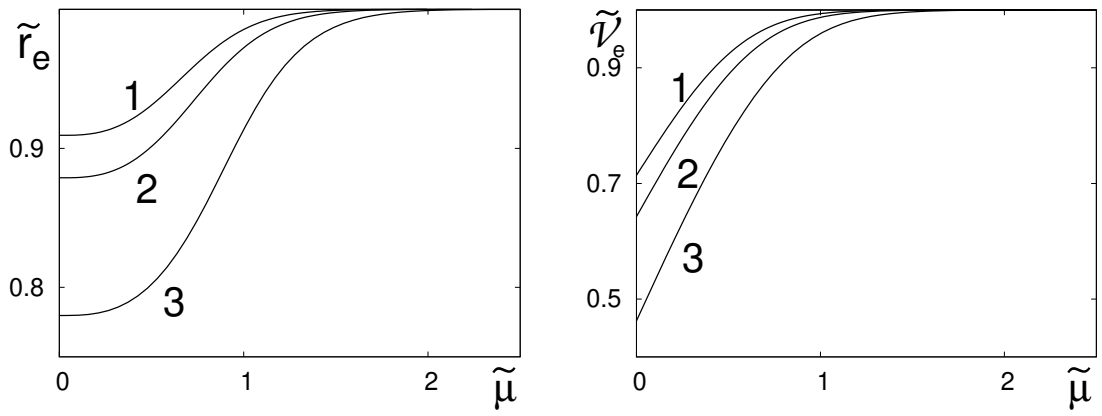

FIG. 5. Plots of the normalized coordinates of the minimum of the effective potential for $\ell = 1$ and $\omega = 1.0, 0.5, 0.1$ – curves 1, 2, 3, respectively, as functions of $\widetilde{\mu}$. In the left panel $\widetilde{r}_{\rm e} \equiv \widetilde{r}_{\rm e}(\ell, \omega, \mu)$; in the right one $\widetilde{\mathcal{V}}_{\rm e} \equiv \widetilde{\mathcal{V}}_{\rm e}(\ell, \omega, \mu)$.

where

$$\mathcal{V}^{\rm h}(r; \ell, \omega) \;=\; \frac{\ell(\ell+1)}{r^2} + \frac{1}{r} + \Big(\frac{\omega\, r}{2}\Big)^2, \tag{42}$$

$$\mathcal{V}^{\rm o}(r; \ell, \omega) \;=\; \frac{\ell(\ell+1)}{r^2} + \Big(\frac{\omega\, r}{2}\Big)^2, \tag{43}$$

are, respectively, the effective potentials of harmonium and of the spherical harmonic oscillator. Since $0 \le \mathsf{w}(r, \mu) \le 1/r$, we have

$$\mathcal{V}^{\rm o}(r; \ell, \omega) \;\le\; \mathcal{V}(r; \ell, \omega, \mu) \;\le\; \mathcal{V}^{\rm h}(r; \ell, \omega). \tag{44}$$

The general shapes of $\mathcal{V}^{\rm o}(r; \ell, \omega)$ and $\mathcal{V}^{\rm h}(r; \ell, \omega)$ are similar: regular potential wells approaching infinity in the same way if $r \to 0$ and $r \to \infty$. Because $\mathsf{w}(r, \mu)$ is regular and monotonic, the shapes of $\mathcal{V}(r; \ell, \omega, \mu)$ are similar. In Fig. 4 plots of $\mathcal{V}(r; \ell, \omega, \mu)$ for $\ell = 1$, $\omega = 1$ (left panel), $\ell = 1$, $\omega = 0.1$ (right panel), and for several values of μ are presented. The ranges of r and $\mathcal{V}$ in the two panels are selected so that the shapes of the curves are similar [the shapes cannot be the same, because $\ell_1 = \ell_2 = 1$, cf. eq. (39)].

If $\ell > 0$ then the effective potential $\mathcal{V}(r; \ell, \omega, \mu)$ has only one extremum: a minimum, at $r = r_{\rm e}(\ell, \omega, \mu)$. The values of $r_{\rm e}$ can be obtained from the condition

$$\left.\frac{\mathcal{V}(r; \ell, \omega, \mu)}{dr}\right|_{r=r_{\rm e}} \;=\; 0,$$

transformed to

$$(r_{\rm e})^4 = \frac{2}{\omega^2}\left[2\ell(\ell+1) + \mu\, r_{\rm e}^2\,\left(\frac{\mathrm{erf}(\mu\, r_{\rm e})}{\mu\, r_{\rm e}} - \frac{2}{\sqrt{\pi}}\,\mathrm{e}^{-(\mu\, r_{\rm e})^2}\right)\right], \tag{45}$$

where $r_{\rm e}$ stands here for $r_{\rm e}(\ell,\omega,\mu)$. Equation (45) has to be solved numerically, but one can see that $r_{\rm e}(\ell,\omega,\mu_1) \geq r_{\rm e}(\ell,\omega,\mu_2)$, if $\mu_1 > \mu_2$. At the limit of $\mu = 0$ (harmonic oscillator),

$$r_{\rm e}^{\rm o}(\ell,\omega)^4 = \frac{4\ell(\ell+1)}{\omega^2}. \tag{46}$$

If $\mu \to \infty$ (harmonium), then $r_{\rm e}^{\rm h}$ is a root of a fourth-order polynomial:

$$r_{\rm e}^{\rm h}(\ell,\omega)^4 = \frac{2}{\omega^2}\left[2\ell(\ell+1) + r_{\rm e}^{\rm h}(\ell,\omega)\right]. \tag{47}$$

The explicit expression is given in [13]. The second coordinate of this minimum is $\mathcal{V}_{\rm e} \equiv \mathcal{V}(r_{\rm e};\ell,\omega,\mu)$, The normalized coordinates of the minimum,

$$\widetilde{r}_{\rm e} \equiv \widetilde{r}_{\rm e}(\ell,\omega,\mu) = \frac{r_{\rm e}(\ell,\omega,\mu)}{r_{\rm e}^{\rm h}(\ell,\omega)}, \quad \text{and} \quad \widetilde{\mathcal{V}}_{\rm e} \equiv \widetilde{\mathcal{V}}_{\rm e}(\ell,\omega,\mu) = \frac{\mathcal{V}(r_{\rm e};\ell,\omega,\mu)}{\mathcal{V}^{\rm h}(r_{\rm e};\ell,\omega)}, \tag{48}$$

are plotted versus $\widetilde{\mu}$ in, respectively, left and right panels of Fig. 5. Similarly as in the case of the model potential (cf. Fig. 1) the minimum of the effective potential is approximately located at its asymptotic position already for $\mu \approx 2\,\mu_0(\omega)$. But, unlike the case of $\ell = 0$, here both $\widetilde{r}_{\rm e}(\ell,\omega,\widetilde{\mu})$ and $\widetilde{\mathcal{V}}_{\rm e}(\ell,\omega,\widetilde{\mu})$ depend on ω.

Finally, the ratio

$$R_\ell(r;\ell,\omega,\mu) = \frac{\mathcal{V}(r;\ell,\omega,\mu)}{\mathcal{V}^{\rm h}(\ell,r;\omega)}, \tag{49}$$

for $\ell = 1$, and for several values of ω and μ is plotted in the right panel of Fig. 3. As in the case of $\ell = 0$, the ω-dependence is noticeable for small values of μ only. The differences between the effective potentials for finite values of μ, and their asymptotic forms is, in the case of $\ell > 0$, much smaller than for $\ell = 0$. This can be seen in Fig. 3: the maximum difference between 1 and R_1 is about three times smaller than between 1 and R_0.

IV. SPECTRUM

At $\mu = 0$ the energy spectrum is given by the well known analytic formula

$$E_{n,\ell}(\omega,0) \;=\; E_{n,\ell}^{\rm o}(\omega) \;=\; \omega\left(2\,n + \ell + \frac{3}{2}\right). \tag{50}$$

According to the Hellmann-Feynman theorem,

$$\frac{\partial\, E_{n,\ell}(\omega,\mu)}{\partial\,\mu} \;=\; \frac{2}{\sqrt{\pi}}\langle\phi_{n,\ell}\left|{\rm e}^{-(\mu\, r)^2}\right|\phi_{n,\ell}\rangle \;\longrightarrow\; \begin{cases} 2/\sqrt{\pi}, & \text{if } \mu = 0, \\ 0, & \text{if } \mu \to \infty. \end{cases} \tag{51}$$

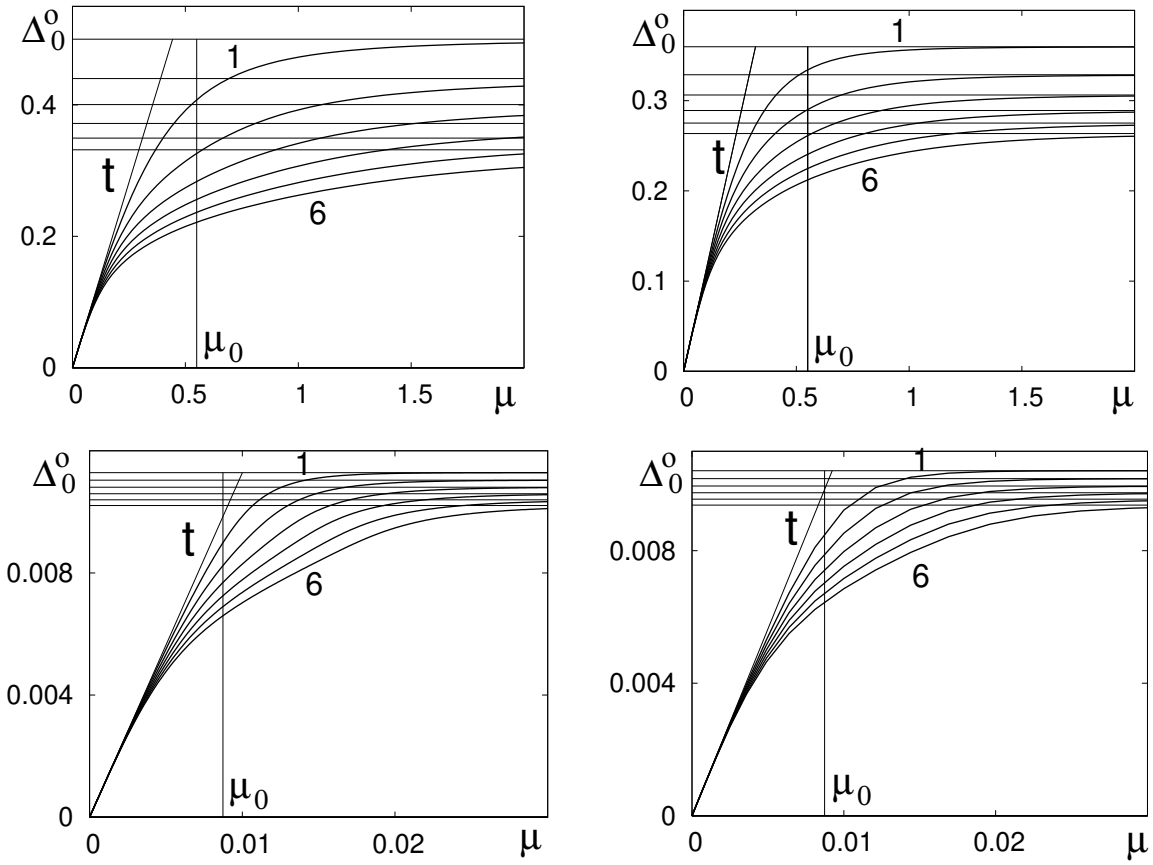

FIG. 6. Plots of Δ_0^o [eq. (53)] expressed in hartrees versus μ (in bohrs^{-1}) for $\omega = 0.5$ (top panels) and $\omega = 0.001$ (bottom panels); $\ell = 0$ (left panels) and $\ell = 1$ (right panels). The vertical lines mark $\mu_0(\omega)$; the tangent lines $t = t(\mu)$ in the bottom-left corners of the panels and the horizontal lines in the upper parts of the panels show the asymptotic behavior of $\Delta_0^o(\mu)$ for $\mu \to 0$ and $\mu \to \infty$, respectively. The upper curves (marked 1) correspond to the ground states and the lowest ones (marked 6) - to the fifth excited states.

Therefore, for a fixed ω, and $\mu \ll 1$,

$$E_{n,\ell}(\omega,\mu) \underset{\mu\to 0}{\to} \frac{2\mu}{\sqrt{\pi}} + E_{n,\ell}(\omega,0) = \frac{2\mu}{\sqrt{\pi}} + \omega\left(2\,n + \ell + \frac{3}{2}\right). \tag{52}$$

Differences

$$\Delta_0^o \equiv \Delta_0^o(n,\ell;\omega,\mu) = E_{n,\ell}(\omega,\mu) - E_{n,\ell}^o(\omega), \tag{53}$$

for $n = 0, 1, \ldots, 6$, $\ell = 0, 1$, and for two values of ω differing by factor 500 ($\omega = 0.5$, and $\omega = 0.001$) are plotted, as functions of μ, in Fig. 6. Though the scaling invariance discussed in previous sections is not valid exactly, one can see that the spectra for different values of

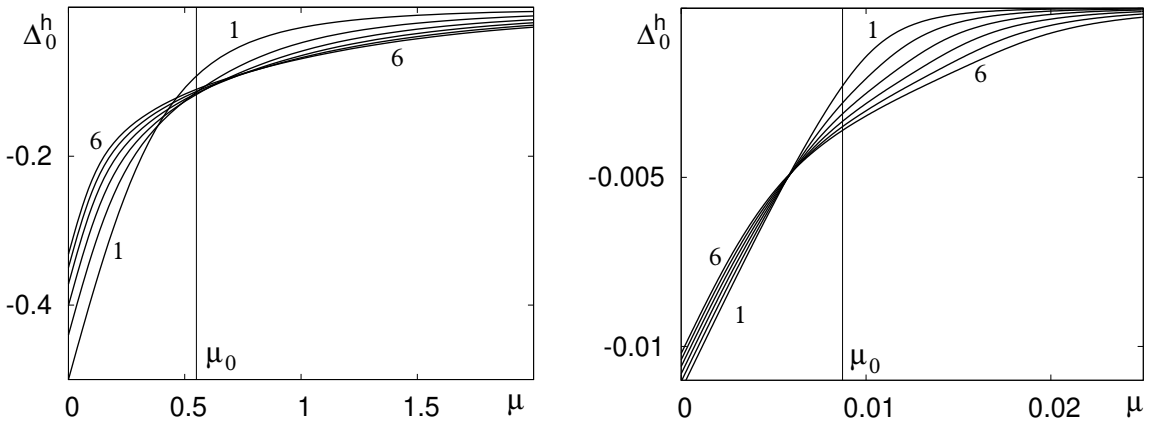

FIG. 7. Plots of Δ_0^{h} [eq. (55)] expressed in hartrees versus μ (in bohrs^{-1}) for $\ell = 0$. Left panel: $\omega = 0.5$; right panel: $\omega = 0.001$. The vertical lines mark $\mu_0(\omega)$. The curves (marked 1) correspond to the ground state and the ones marked 6 - to the fifth excited state.

the confinement parameter have similar structure.

The average distance between electrons, $\langle\, r \,\rangle$, in the case of the harmonic oscillator, is proportional to $1/\sqrt{\omega}$. This kind of dependence is approximately valid for a broad range of ω. The increasing repulsion between electrons (increasing μ) leads to an increase of $\langle\, r \,\rangle$. In the case of $\omega = 0.001$ the average distance between electrons is of the order of 100 bohrs, increasing from about 50 bohrs at the limit of the harmonic oscillator to 130 bohrs at the limit of harmonium. In such cases the influence of the centrifugal term, proportional to $1/r^2$, is small – for small r the wave function is close to 0. This can be seen by comparing the left and the right panels in Fig. 6: a difference is visible if $\omega = 0.5$, but if $\omega = 0.001$, then the plots for $\ell = 0$ and for $\ell = 1$ are nearly the same – the relative difference between the ground state energies of $\ell = 0$ and $\ell = 1$ is, in the case of $\omega = 0.001$, about 1%. The range of the validity of the linear approximation (52) can be estimated for small μ by comparing the tangent lines

$$t(\mu) \,=\, \frac{2\,\mu}{\sqrt{\pi}} \tag{54}$$

with the curves representing the exact energies.

The energy of harmonium can be expressed analytically only in some special cases, but the structure of its spectrum is well known (see e.g. [14]). As a function of ω, the spectrum can be divided to three parts: (1) $\omega \,>\, 1$ – strong confinement dominates the Coulomb interaction, the electron correlation is weak and we have the harmonic oscillator regime;

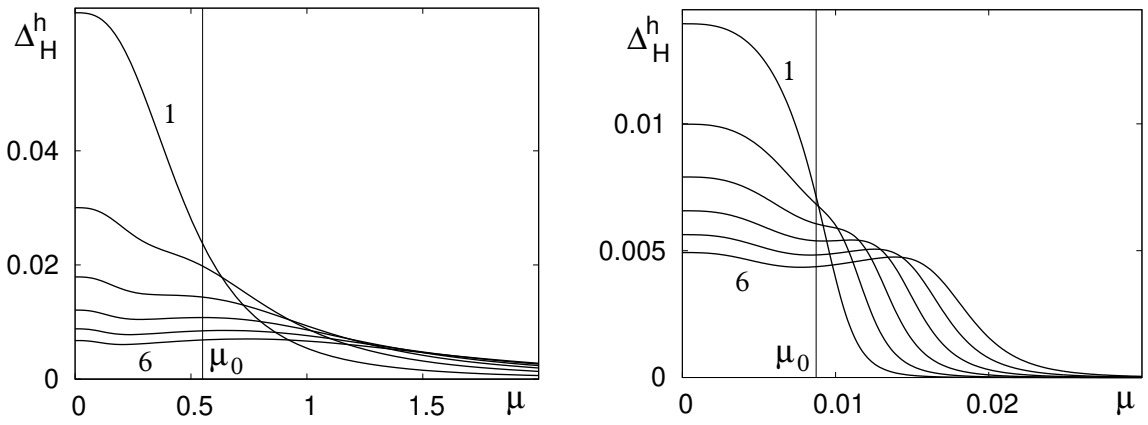

FIG. 8. Plots of $\Delta^{\rm h}_{\rm H} \equiv \Delta^{\rm h}_{\rm H}(n,\ell;\omega,\mu)$ [eq. (56)] expressed in hartrees versus μ (in bohrs^{-1}), for $\omega = 0.5$ (left panel) and $\omega = 0.001$ (right panel), and $\ell = 0$. The vertical lines mark $\mu_0(\omega)$. The curves marked 1 correspond to the ground state and the ones marked 6 - to the fifth excited state.

(2) $\omega \in (10^{-5}, 1)$ – the intermediate regime, the relation between the confinement and the Coulomb interaction is, in a sense, similar as in atoms; (3) $\omega < 10^{-5}$ – very weak confinement, the electrons are far apart and their motion is strongly correlated. Differences

$$\Delta^{\rm h}_0 \equiv \Delta^{\rm h}_0(n,\ell;\omega,\mu) = E_{n,\ell}(\omega,\mu) - E^{\rm h}_{n,\ell}(\omega), \tag{55}$$

for $n = 0, 1, \ldots, 6$, $\ell = 0$, and $\omega = 0.5$, 0.001 are plotted, as functions of μ, in Fig. 7. Similarly as in the diagrams presented in Fig. 6, also here one can see a qualitative change of the spectrum when $\mu \approx \mu_0(\omega)$. In the case of the harmonic oscillator the distances between the neighboring energy levels, for given ℓ and ω, are constant (independent of n). In the case of harmonium, these distances increase with increasing n [14]. When μ changes from the large to the small values, the distances between the energy levels gradually change from the mode of harmonium to the mode of harmonic oscillator. This can be seen in Fig. 7 – in the area $\mu \approx \mu_0(\omega)$, the order of the values of $\Delta^{\rm h}_0$ in terms of n, changes to the reverse.

As it was already mentioned, using the smooth long-range interaction potential instead of the singular Coulomb one, reduces the computational effort in the approximate solving the Schrödinger equation for many-electron systems [1–3]. Therefore, one of the objectives of studying properties of erfonium, is an exploration of the possibility of an extrapolation of the energy derived from a model with a finite μ to the limit of electrons interacting by the Coulomb force, i.e. the transition from the spectrum of a finite-μ erfonium to the spectrum

of harmonium. The first step in such a procedure is the approximation of the energies of harmonium by the expectation values of the harmonium Hamiltonian calculated using the wave functions of erfonium [4]. The resulting correction to the energy, equal to

$$\Delta^{\rm h}_{\rm H} \equiv \Delta^{\rm h}_{\rm H}(n,\ell;\omega,\mu) = \langle\, \phi_{n,\ell}(\mu)|\mathsf{H}^{\rm h}|\phi_{n,\ell}(\mu)\,\rangle - E^{\rm h}_{n,\ell}(\omega), \tag{56}$$

where

$$\langle\, \phi_{n,\ell}(\mu)|\mathsf{H}^{\rm h}|\phi_{n,\ell}(\mu)\,\rangle \equiv \langle\, \phi_{n,\ell}(r;\omega,\mu)|\mathsf{H}(r;\ell,\omega,\infty)|\phi_{n,\ell}(r;\omega,\mu)\,\rangle,$$

is plotted in Fig. 8. As one can see by comparing with Fig. 7, the difference between $\left|\Delta^{\rm h}_0\right|$ and $\left|\Delta^{\rm h}_{\rm H}\right|$ depends on the value of ω. If ω is large (left panels), then $\left|\Delta^{\rm h}_{\rm H}\right| \ll \left|\Delta^{\rm h}_0\right|$ (for $\omega = 0.5$ by factor ≈ 10). But if ω is small (right panels), then both differences are of the same order of magnitude.

The difference between $E_{n,\ell}(\omega,\mu)$ and $E^{\rm h}_{n,\ell}(\omega)$ can be dramatically reduced if the generalized cusp conditions are used to represent the wave function at small r. But, if μ is smaller than a certain threshold, a further reduction of the difference using this method proved to be impossible [4]. From the perspective of the present analysis it is understandable that the threshold value is close to $\mu_0(\omega)$, where the character of the potential (and of the spectrum) changes from a harmonium-like to an oscillator-like.

V. FINAL REMARKS

Erfonium, a Hooke atom with a soft interaction potential represented by $\mathrm{erf}(\mu\, r)/r$, makes a bridge between harmonium ($\mu \to \infty$) and the spherical harmonic oscillator ($\mu = 0$). The parameter μ establishes an adiabatic connection between these two limits. An interplay between the effects specific for harmonium and for the harmonic oscillator creates a rich and interesting pattern which can be observed in the structure of the potential and of the spectrum. The parameter $\mu_0(\omega)$ determined by the strength of the confinement (27), marks a fuzzy boundary between these two "spheres of influence". If $\mu > \mu_0(\omega)$ then the regime of harmonium dominates, if $\mu < \mu_0(\omega)$, then the features of the harmonic oscillator prevail.

A vast field for further studies remains open. Particularly interesting (and difficult) are issues related to the behavior of erfonium at the limit of $\omega \to 0$. Notice that at this limit the spectrum abruptly changes from entirely discrete, to entirely continuous. If simultaneously $\mu \to 0$, then at the limit we get two unconfined and non-interacting 'electrons'.

Last, but not least, a broad class of semi-analytic (cf. [12, 13]) and variational approaches may result in precise analytic approximations of the wave functions and of the energies of erfonium.

Acknowledgement

We thank Prof. Henryk A. Witek (National Chiao Tung University, Hsinchu, Taiwan) for his constructive remarks and for useful discussions.

ORCID

Jacek Karwowski: https://orcid.org/0000-0003-1508-2929
Andreas Savin: https://orcid.org/0000-0001-8401-8037

[1] P. Gori-Giorgi and A. Savin, "Properties of short-range and long-range correlation energy density functionals from electron-electron coalescence," Phys. Rev. A **73**, 032506 (2006).

[2] A. Savin, "Correcting model energies by numerically integrating along an adiabatic connection and a link to density functional approximations," J. Chem. Phys. **134**, 214108 (2011).

[3] A. Savin, "Models and corrections: Range separation for electronic interaction – Lessons from density functional theory," J. Chem. Phys. **153**, 160901 (2020).

[4] A. Savin and J. Karwowski, "Correcting models with long-range electron interaction using generalized cusp conditions," J. Phys. Chem. A **127**, 1377–1385 (2023).

[5] C. E. González-Espinoza, P. W. Ayers, J. Karwowski, and A. Savin, "Smooth models for the coulomb potential," Theor. Chem. Acc. **135**, 256 (2016).

[6] K. Pernal and M. Hapka, "Range-separated multiconfigurational density functional theory methods," WIREs Comput. Mol. Sci. **12**, e1566 (2022).

[7] P. P. Ewald, "Die berechnung optischer und elektrostatischer gitterpotentiale (the calculation of optical and electrostatic grid potential)," Ann. Phys (Leipzig) **369**, 253–287 (1921).

[8] G. S. Demyanov and P. R. Levashov, "Systematic derivation of angular-averaged ewald potential," J. Phys. A: Math. Theor. **55**, 385202 (2022).

[9] W. Lucha, H. Rupprecht, and F. F. Schoeberl, "Significance of relativistic wave equations for bound states," Phys. Rev. D **46**, 1088–1095 (1992).

[10] R. Plamondon, "General relativity: An erfc metric," Results in Physics **9**, 456–462 (2018).

[11] N. R. Kestner and O. Sinanoglu, "Study of electron correlation in helium-like systems using an exactly soluble model," Phys. Rev. **128**, 2687 (1962).

[12] M. Taut, "Two electrons in an external oscillator potential: Particular analytic solutions of a coulomb correlation problem," Phys. Rev. A **48**, 3561–3566 (1993).

[13] S. Mandal, P. K. Mukherjee, and G. H. F. Diercksen, "Two electrons in a harmonic potential: an approximate analytical solution," J. Phys. B: At. Mol. Opt. Phys. **36**, 4483–4494 (2003).

[14] J. Karwowski and L. Cyrnek, "Harmonium," Ann. Phys. (Leipzig) **13**, 181 – 193 (2004).